Journal of Controlled Release 208 (2015) 121–129

Contents lists available at ScienceDirect

Journal of Controlled Release

journal homepage: www.elsevier.com/locate/jconrel

Cationic liposome–hyaluronic acid hybrid nanoparticles for intranasal vaccination with subunit antigens

Yuchen Fan [a,b,1], Preety Sahdev [a,b,1], Lukasz J. Ochyl [a,b], Jonathan J. Akerberg [a,b], James J. Moon [a,b,c,*]

[a] Department of Pharmaceutical Sciences, University of Michigan, Ann Arbor, MI 48109, USA
[b] Biointerfaces Institute, University of Michigan, Ann Arbor, MI 48109, USA
[c] Department of Biomedical Engineering, University of Michigan, Ann Arbor, MI 48109, USA

ARTICLE INFO

Article history:
Received 16 December 2014
Received in revised form 5 April 2015
Accepted 9 April 2015
Available online 11 April 2015

Keywords:
Liposome
Nanoparticle
Subunit antigen
Intranasal vaccine
Yersinia pestis

ABSTRACT

Here we report the development of a new cationic liposome–hyaluronic acid (HA) hybrid nanoparticle (NP) system and present our characterization of these NPs as an intranasal vaccine platform using a model antigen and F1-V, a candidate recombinant antigen for *Yersinia pestis*, the causative agent of plague. Incubation of cationic liposomes composed of DOTAP and DOPE with anionic HA biopolymer led to efficient ionic complexation and formation of homogenous liposome–polymer hybrid NPs, as evidenced by fluorescence resonance energy transfer, dynamic light scattering, and nanoparticle tracking analyses. Incorporation of cationic liposomes with thiolated HA allowed for facile surface decoration of NPs with thiol-PEG, resulting in the formation of DOTAP/HA core-PEG shell nanostructures. These NPs, termed DOTAP–HA NPs, exhibited improved colloidal stability and prolonged antigen release. In addition, cytotoxicity associated with DOTAP liposomes (LC_{50} ~ 0.2 mg/ml) was significantly reduced by at least 20-fold with DOTAP–HA NPs (LC_{50} > 4 mg/ml), as measured with bone marrow derived dendritic cells (BMDCs). Furthermore, NPs co-loaded with ovalbumin (OVA) and a molecular adjuvant, monophosphoryl lipid A (MPLA) promoted BMDC maturation and upregulation of co-stimulatory markers, including CD40, CD86, and MHC-II, and C57BL/6 mice vaccinated with NPs via intranasal route generated robust OVA-specific $CD8^+$ T cell and antibody responses. Importantly, intranasal vaccination with NPs co-loaded with F1-V and MPLA induced potent humoral immune responses with 11-, 23-, and 15-fold increases in F1-V-specific total IgG, IgG_1, and IgG_{2c} titers in immune sera by day 77, respectively, and induced balanced Th1/Th2 humoral immune responses, whereas mice immunized with the equivalent doses of soluble F1-V vaccine failed to achieve sero-conversion. Overall, these results suggest that liposome–polymer hybrid NPs may serve as a promising vaccine delivery platform for intranasal vaccination against *Y. pestis* and other infectious pathogens.

1. Introduction

Synthetic nanoparticles (NPs) are promising delivery systems for subunit vaccines composed of peptides, recombinant proteins, or DNA [1–3]. Advantages of particulate vaccines include efficient encapsulation of antigens, shielding of antigens from rapid enzymatic degradation, and ability to co-deliver antigens with molecular adjuvants to antigen-presenting cells (APCs), thus promoting cellular and humoral immune responses [3]. Among particulate vaccine delivery systems, liposomes of various lipid compositions have been widely investigated as potential vaccine carriers. In particular, cationic liposomes composed of 1,2-dioleoyl-3-trimethylammonium-propane (DOTAP) have been extensively studied as they can readily form nano-complexes with anionic peptides, proteins, and plasmid DNA encoding for antigens and generate T and B cell immune responses in vivo [4–8]. Despite significant advances made in this field, there are still several major challenges remaining for liposomal vaccines, including cytotoxicity of cationic liposomes that can negatively impact immune responses at high concentrations as well as their suboptimal in vivo stability for delivery of biomacromolecules [6–10]. We previously addressed some of these issues by developing a new lipid-based NP system formed by divalent cation-induced liposomal fusion into multilamellar vesicles and subsequent cross-linking of apposing lipid layers via maleimide–thiol reaction [11]. The resulting NPs released cargo protein in a stable manner and elicited robust humoral and cellular immune responses [11–13]. As an alternative approach to producing stable vaccine delivery systems, here we aimed to synthesize lipid–biopolymer hybrid NPs by exploiting ionic charge interactions between liposomes and hyaluronic acid (HA), which is a biodegradable polymer that has been shown to form complexes with liposomes [14] and investigated as a vaccine delivery agent [15–17]. Specifically, we utilized ionic complexation between cationic DOTAP-based liposomes and anionic HA-based biopolymers to form DOTAP–HA hybrid NPs, which were then surface-decorated with poly(ethylene glycol) (PEG), resulting in the

* Corresponding author at: 2800 Plymouth Road NCRC, Ann Arbor, MI 48109, USA.
E-mail address: moonjj@umich.edu (J.J. Moon).
[1] The authors contributed equally to this work.

http://dx.doi.org/10.1016/j.jconrel.2015.04.010
0168-3659/

formation of DOTAP/HA core-PEG shell NPs. We report here that these NPs may serve as a promising vaccine delivery platform for intranasal vaccination.

Yersinia pestis, a causative agent of pneumonic plague, is a Category A bioterrorism bacterial agent that can be easily transmitted through pulmonary inhalation, potentially causing a death rate near 100% within a week of infection [18]. However, there are currently no available vaccine products against pneumonic plague. Therefore, it is of high priority to develop a protective plague vaccine. For vaccination against *Y. pestis*, intranasal route of immunization is attractive due to ease of vaccine administration and rapid deployment in the time of imminent biological threat. In addition, nasal cavity is characterized by highly permeable nasal epithelium for absorption of biomolecules and high frequency of immune cells within nasal-associated lymphoid tissues [19]. Thus, nasal vaccination against *Y. pestis* may drive induction of local mucosal immune responses in the airway to prevent initial pneumonic infection while simultaneously eliciting systemic immune responses to inhibit transmission of bacterial infection. In particular, F1-V, a recombinant fusion protein of fraction 1 pilus and LcrV antigen from *Y. pestis*, has been demonstrated to be a promising candidate for plague vaccine in a number of previous studies [18,20]. In addition, F1-V in combination with various types of adjuvants [21] or nanocarriers [22,23] has been shown to promote prophylactic humoral immune responses against *Y. pestis*.

In this study, we report the development of a new liposome–polymer hybrid NP system and our initial characterization of these NPs as an intranasal vaccine platform using a model antigen as well as F1-V. We show that DOTAP liposomes can be readily incorporated with thiolated HA (HA-SH) by promoting ionic complexation between DOTAP and HA-SH. The resulting DOTAP–HA NPs were further stabilized by reacting the HA-SH layer on the outer shell with thiolated PEG (PEG-SH), generating stable DOTAP/HA core-PEG shell NPs (Fig. 1). Importantly, cytotoxicity of DOTAP liposomes in BMDCs (LC_{50} ~ 0.2 mg/ml) was significantly reduced by at least 20-fold (LD_{50} > 4 mg/ml) for DOTAP–HA NPs. In addition, toll-like receptor (TLR) 4 agonist, MPLA [24], was chosen as a molecular adjuvant for both the model antigen OVA and F1-V. DOTAP–HA hybrid NPs co-loaded with antigens and MPLA promoted maturation of BMDCs in vitro and effectively stimulated antigen-specific cellular and humoral immune responses in vivo after intranasal vaccination, suggesting their potency as a promising nasal vaccine platform against infectious pathogens.

2. Materials and methods

2.1. Reagents

Lipids including 1,2-dioleoyl-3-trimethylammonium propane (DOTAP), 1,2-dioleoyl-sn-glycero-3-phosphoethanolamine (DOPE), nitrobenzoxadiazole (NBD)-labeled DOPE (DOPE-NBD), rhodamine (Rhod)-labeled DOPE (DOPE-Rhod), and MPLA were all purchased form Avanti Polar Lipids (Alabaster, AL). Sodium hyaluronate (HA) and 2 kDa PEG-SH were from Lifecore Biomedical (Chaska, MN) and Laysan Bio (Arab, AL), respectively. L-cysteine, N-(3-Dimethylaminopropyl)-N′-ethylcarbodiimide hydrochloride (EDC), N-hydroxysuccinimide (NHS), 5,5′-Dithiobis(2-nitrobenzoic acid) (DTNB) and chloramine T were obtained from Sigma-Aldrich (St. Louis, MO). Ovalbumin (OVA) and F1-V were obtained from Worthington (Lakewood, NJ) and NIH BEI Resources (Manassas, VA), respectively. RPMI 1640 media, fetal bovine serum (FBS), penicillin–streptomycin, β-mercaptoethanol, ACK lysis buffer and Texas Red N-hydroxysuccinimide ester were from Life Technologies (Grand Island, NY). Granulocyte macrophage colony stimulating factor (GM-CSF) was the product of PeproTech (Rocky Hill, NJ). Rat anti-mouse CD16/32, CD86-PE, CD40-APC, and MHC Class II-FITC were from eBioscience (San Diego, CA). Rat anti-mouse CD8-APC, hamster anti-mouse CD11c-PE-

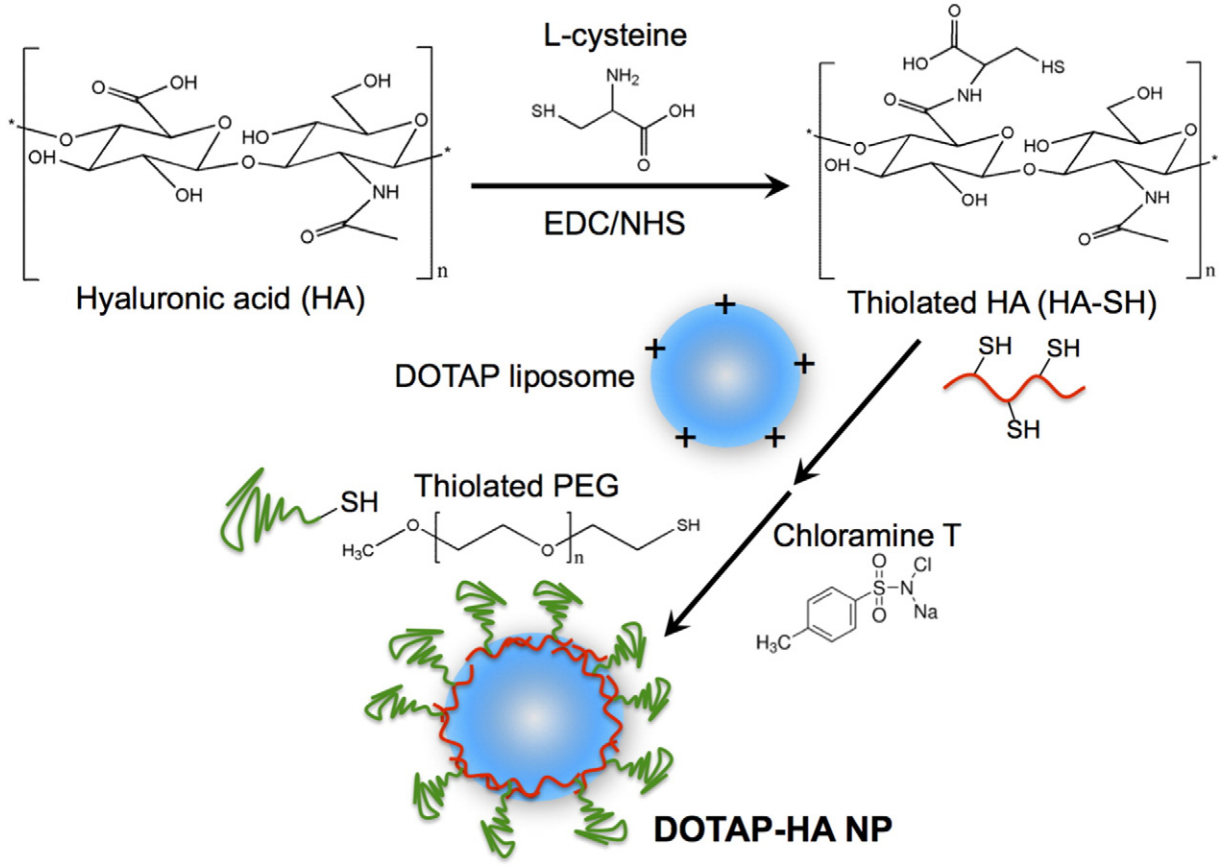

Fig. 1. Schematic illustration of thiolation of hyaluronic acid and formation of lipid–polymer hybrid nanoparticles.

Cy7 were from BD Bioscience (San Jose, CA). iTAg tetramer/PE — H-2 Kb OVA (SIINFEKL) was purchased from Beckman Coulter (Brea, CA). Zymax Rabbit anti-mouse IgG and HRP Rat anti-mouse IgG_1 were purchased from Invitrogen (Grand Island, NY), and Goat anti-mouse IgG_{2c} was from Southern Biotech (Birmingham, AL). 3.3′,5.5′-tetramethylbenzidine (TMB) substrate solution was purchased from Thermo Scientific (Waltham, MA).

2.2. Thiolation of hyaluronic acid

Thiolated HA was synthesized by conjugation of HA with L-cysteine via EDC/NHS reaction. Briefly, 200 mg HA was dissolved by 20 ml deionized water containing 200 mM EDC and NHS. The pH was then adjusted to 5 with 1 M HCl. The reaction mixture was stirred for 0.5 h, followed by addition of 400 mg L-cysteine and stirring at room temperature for another 4 h. The thiolated HA (HA-SH) was purified by dialysis (MWCO 10 kDa) against dilute HCl (pH 5), 0.9% NaCl in dilute HCl, and then dilute HCl again. Finally, the dialyzed sample was lyophilized and stored at −80 °C. The free thiol content of HA-SH was measured by Ellman's assay as previously reported [16,17].

2.3. Preparation of liposomes and liposome–polymer hybrid NPs

DOTAP and DOPE (each 0.5 mg) were dissolved in chloroform, followed by solvent evaporation to form lipid film. The dried lipid film was hydrated with 0.2 ml deionized water at room temperature for 1 h with intermittent vortex, followed by addition of varying amounts of HA or HA-SH and incubation for 1 h. Next, 0.1 ml PEG-SH solution (5 mg/ml in 10 mM HEPES buffer, pH 7.4) was added and the pH was adjusted to 8 with 1 M sodium hydroxide. Then 50 μl of chloramine T solution (50 mM in HEPES buffer, pH 7.4) was added to induce thiol-mediated conjugation of PEG-SH onto HA-SH. After 1 h incubation at room temperature, the resulting particles were collected by centrifugation at 20,000 × *g* for 10 min, washed with PBS, resuspended in 0.2 ml PBS, briefly sonicated, and stored at 4 °C till use. In some cases, the initial lipid film was prepared along with 2.9 μg of MPLA, and hydrated with solution containing 200 μg of OVA to synthesize OVA/MPLA-loaded DOTAP–HA NPs. Since MPLA with hydrophobic acyl chains has been previously shown to be efficiently incorporated into liposomes and lipid-based nanoparticles via self-assembly into lipid membranes [11,25], we assumed 100% loading efficiency for MPLA in DOTAP–HA NPs. Encapsulation efficiency of OVA into NPs was determined to be 11 ± 1.8%, as assessed by running the samples through SDS-PAGE, followed by Coomassie staining and densiometry measurement.

Particle samples were diluted with deionized water or PBS, followed by size and zeta potential measurements by dynamic light scattering (DLS, Zetasizer Nano ZSP, Malvern, UK). In addition, detailed NP size distribution and NP concentration were obtained by nanoparticle tracking analysis (NTA, NanoSight NS300, Malvern, UK) as reported previously [26]. PEG content in the final particle was determined by complexation of PEG with barium iodide as reported previously [27,28]. Briefly, 200 μl of 5% (w/v) barium chloride dissolved by 1 M hydrochloride acid and 100 μl of iodide solution containing 0.05 M iodine and 2% (w/v) potassium iodide were added to 800 μl of ×200 diluted particle suspension, followed by an incubation at room temperature for 15 min. Absorbance at 535 nm was measured for PEG quantification. The dry weight of particles after lyophilization was measured to report the PEG content in μmol/g of particles. For the in vitro release study, OVA was labeled with Texas Red N-hydroxysuccinimide ester and encapsulated into DOTAP–HA NPs. NPs were resuspended in phenol red-free RPMI 1640 supplemented with 10% FBS, loaded in dialysis cassettes (MWCO 300 kDa), and incubated at 37 °C under constant shaking. Release media were collected at pre-determined time points during 3 weeks, followed by fluorescence measurement with excitation and emission wavelengths of 585/615 nm using a microplate fluorometer (Synergy Neo, BioTek, USA). The extent of polymer-induced liposomal fusion was assessed by the fluorescence resonance energy transfer (FRET) method [29,30]. Briefly, liposomes incorporating 5 mM DOPE-NBD (donor) or DOPE-Rhod (acceptor) were prepared separately, then mixed at 1:1 volume ratio, followed by addition of varying amounts of HA. After incubation at room temperature for 1 h, the samples were diluted 200 times and fluorescence intensity was measured by a microplate fluorometer with excitation at 480 nm and emission filters set at 540 nm and 600 nm. FRET index was calculated as fluorescence intensity at 600 nm divided by that at 540 nm [31].

2.4. Preparation of BMDCs

BMDCs were prepared as described previously [32]. Briefly, femur and tibia were harvested from C57BL/6 mice, and cells were collected by flushing bone marrow with a syringe and passing the cell suspension through a cell strainer (mesh size = 40 μm). After centrifugation, cells were seeded into non-tissue culture treated petri-dish at a density of 2×10^6 cells/dish and cultured in DC culture media (RPMI 1640 supplemented with 10% FBS, 1% penicillin–streptomycin, 50 μM β-mercaptoethanol, and 20 ng/ml GM-CSF) at 37 °C with 5% CO_2. Culture media were refreshed on days 3, 6 and 8, and BMDCs were used on days 10–12.

2.5. Activation and viability of BMDCs

BMDCs were seeded at a density of 8×10^5 cells/ml into 12-well plates and cultured overnight. Cells were incubated with culture media, liposomes, or liposome–polymer hybrid NPs encapsulating 5 μg/ml of OVA, with or without 0.58 μg/ml of MPLA at 37 °C for 2 h, followed by washing with PBS and overnight culture. BMDCs were harvested, incubated with anti-CD16/32 at room temperature for 10 min, and then stained with fluorescent probe-labeled antibodies against CD11c, CD40, CD86, and MHC II at room temperature for 30 min. Finally, cells were washed and resuspended in 2 μg/ml DAPI solution and analyzed by flow cytometry (Cyan 5, Beckman Coulter, USA). BMDC viability following different treatments was measured by CCK-8 kit [33]. Briefly, BMDCs were seeded into 96-well plates (40,000 cells/well) and cultured overnight. Cells were then incubated with liposomes or liposome–polymer hybrid NPs encapsulating OVA, with or without MPLA, with various lipid concentrations. Following 2 h incubation at 37 °C, cells were washed by PBS and cultured overnight. Finally, cells were incubated with CCK-8 reagent for 2 h at 37 °C and OD450 was measured with a microplate reader.

2.6. In vivo immunization studies

All in vivo experiments were performed under approval from Institutional Animal Care and Use Committee (IACUC) at University of Michigan. Female, 6-week old C57BL/6 mice (The Jackson Laboratory, USA) were randomly divided into 3 groups (n = 3–7) and administered with PBS, OVA plus MPLA solution, or hybrid NPs co-encapsulating OVA and MPLA via intranasal route of immunization. Intranasal vaccination was performed by anesthetizing mice with isoflurane and administering both nostrils with a total vaccine dose of 50 μg of OVA and 0.58 μg of MPLA in 20–40 μl per mouse. A booster dose was given on day 28 after the prime vaccination. Sera samples were collected on days 21 and 49 for ELISA analysis. We also assessed the frequency of OVA-specific $CD8^+$ T cells among peripheral blood mononuclear cells (PBMCs) on day 7 post-vaccination as we recently reported [34]. Briefly, blood samples were collected by retro-orbital bleeding, lysed with ACK lysis buffer, followed by centrifugation to collect pellets, which were then blocked by CD16/32 blocking antibody and incubated with PE labeled SIINFEKL tetramer for 30 min on ice. Samples were then incubated with anti-CD8-APC for 20 min on ice. Cells were washed and resuspended in 2 μg/ml DAPI solution for analysis by flow cytometry.

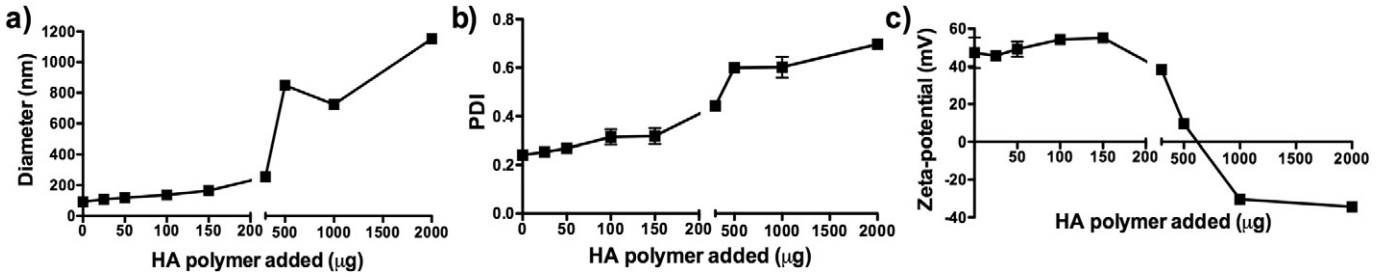

Fig. 2. Characterization of liposomes interacting with varying amounts of HA polymer. HA in varying amounts was added per 1 mg of DOTAP:DOPE liposomes, and particle size (a), PDI (b) and zeta potential (c) were measured. Results are reported as mean ± SEM (n = 3).

In vivo biodistribution of antigen was investigated by injecting C57BL/6 mice (n = 3 per group) with PBS or 50 μg of Texas Red-labeled OVA either in free soluble or NP forms via intranasal or intravenous tail vein administration, and visualizing fluorescence signal from the major organs (e.g. heart, lungs, spleen, liver, and kidneys) with a Xenogen IVIS Spectrum Imaging System at 4 h post-administration.

For studies with F1-V, mice (n = 4) were intranasally immunized with F1-V plus MPLA solution or hybrid NPs co-encapsulating F1-V and MPLA. The doses for prime vaccination on day 0 and 1st booster vaccination on day 28 were 1 μg F1-V and 0.58 μg MPLA per mouse, while the 2nd booster dose given on day 56 was increased to 5 μg F1-V and 2.9 μg MPLA per mouse. Sera samples were collected on days 0, 7, 21, 35, 49, 63 and 77 post the prime dose.

2.7. Enzyme linked immunosorbent assay (ELISA)

ELISA was used to determine sera anti-OVA or anti-F1-V antibody titers post-immunization. Microtiter plate was coated with OVA (1 μg/well) or F1-V (200 ng/well) dissolved in carbonate–bicarbonate buffer (pH 9.6) at 4 °C overnight. Wells were washed and blocked by 1% BSA for 2 h, followed by incubation with serially diluted sera at room temperature for 1 h, incubation with HRP-conjugated anti-IgG, IgG_1 or IgG_{2c} for another hour, and colorization with TMB substrate solution for 5 min. The reaction was stopped by 2 M H_2SO_4, and absorbance at 450 nm was measured by a microplate reader.

2.8. Statistical analysis

Data were analyzed by one- or two-way analysis of variance (ANOVA), followed by Bonferroni's test for comparison of multiple groups with Prism 5.0 (GraphPad Software). *p* values less than 0.05 were considered statistically significant. All values are reported as means ± SEM with at least triplicate data points.

3. Results

3.1. Lipid–polymer hybrid NPs formed by ionic complexation of DOTAP liposomes and HA

Liposome–polymer hybrid NPs were synthesized by utilizing ionic complexation of positively charged liposomes and negatively charged HA. As shown in Fig. 2a, the initial liposomes hydrated from lipid films composed of DOTAP and DOPE (henceforth referred to as DOTAP liposomes) had the particle size of 91.4 ± 0.4 nm. As an increasing amount of HA was added to the unilamellar liposomes, their size gradually increased, reaching 164.0 ± 1.4 nm with 150 μg HA added per 1 mg of liposome suspension. Addition of more than 300 μg of HA caused non-homogeneous aggregation shown by abrupt increase in particle sizes (Fig. 2a) and PDI values (Fig. 2b). Similarly, zeta potential of the lipid–polymer hybrid particles maintained values ranging from 47 to 55 mV with 0–150 μg HA added per 1 mg of liposome suspension (Fig. 2c). Addition of ≥300 μg of HA sharply decreased the surface charge of lipid–polymer hybrid particles, with their zeta potential readings reaching negative values with HA ≥ 1000 μg.

Ionic complexation between DOTAP liposomes and HA biopolymer was further assessed by FRET assay, in which the efficiency of resonance energy transfer was measured between fluorescent NBD- (donor) and rhodamine- (acceptor) lipids initially on separate DOTAP liposomes and intermixed after addition of varying amounts of HA. As shown in Fig. 3, addition of even 25 μg HA into liposomal suspension efficiently induced fusion of liposomes. The extent of fusion was decreased when more than 150 μg of HA was added to the batch of liposomes, suggesting that excess HA with anionic charge may reduce the extent of liposomal fusion by coating the external surfaces of cationic DOTAP liposomes. Based on the ability to induce ionic complexation between DOTAP liposomes and HA and form lipid–polymer hybrid NPs with homogeneous size, we chose to synthesize the hybrid NPs with 100 μg of HA for the subsequent studies.

3.2. PEGylated DOTAP–HA NPs exhibit colloidal stability and allow steady antigen release

In order to coat the external surfaces of liposome–HA hybrid particles with hydrophilic PEG shell, we introduced free sulfhydryl groups to HA by EDC-mediated reaction between carboxylic groups in HA and amine group in L-cysteine (Fig. 1). Ellman's assay indicated that thiolated HA contained 313.8 ± 1.8 μmol/g of free sulfhydryl groups. Analyses of DOTAP liposomes incorporated with varying amounts of thiolated HA showed similar trends in terms of particle size, PDI, and zeta potential values as in Fig. 2 (data not shown), indicating that introduction of sulfhydryl groups in HA did not significantly alter the ability

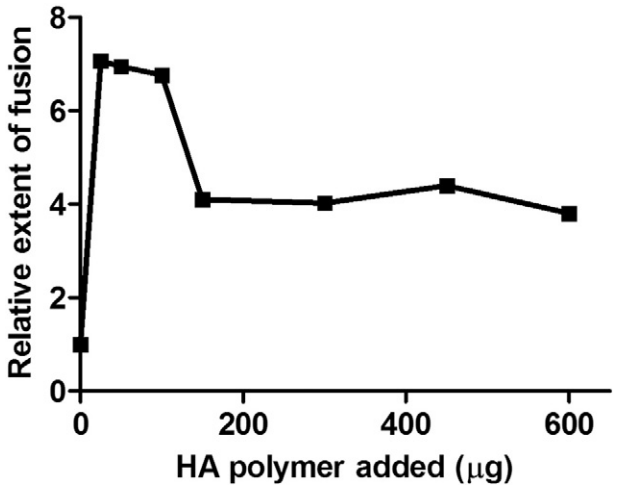

Fig. 3. Ionic complexation of DOTAP liposomes and HA. DOTAP liposomes were separately prepared with NBD- or Rhod-labeled lipid, followed by addition of various amounts of HA. The efficiency of FRET was measured with respect to the control liposomes without HA. Results are means ± SEM (n = 3).

Table 1
Characterization of DOTAP–HA NPs. Results are reported as mean ± SEM (n = 3).

	Size (nm)	PDI	Zeta potential (mV)	PEGylation efficiency (%)	PEG content (μmol/g particle)
Blank DOTAP–HA NPs	190 ± 1.3	0.184 ± 0.002	−16.8 ± 0.07	24 ± 5	47 ± 4
OVA-loaded DOTAP–HA NPs	250 ± 12	0.247 ± 0.005	−15.1 ± 0.9	22 ± 0.9	51 ± 13

of biopolymer to form complexation with DOTAP liposomes. DOTAP liposomes incorporated with 100 μg of thiolated HA were PEGylated by incubation with 2 kDa MW thiol-PEG in the presence of an oxidizing agent, chloramine T, and the resulting NPs (henceforth referred to as DOTAP–HA NPs) were analyzed for their size and surface charge with Zetasizer Nano, as presented in Table 1. We measured the PEG content in DOTAP–HA NPs by assessing complexation of PEG with barium iodide as reported previously [27,28], and the results indicated that ~24% of thiol-PEG initially added to the particle suspension was conjugated on the surfaces of DOTAP–HA NPs with PEG concentration of 47 ± 4 μmol per gram of particles (Table 1). We also carried out similar assays with DOTAP–HA NPs loaded with OVA, and the results showed that incorporation of OVA led to modest increases in particle size and PDI, whereas PEGylation efficiency and PEG content remained similar.

In addition, we performed more detailed size distribution analyses on DOTAP–HA NPs with nanoparticle tracking analysis (NTA), which has been reported to be a more accurate analytical tool than DLS analysis for assessing particle size distribution [26]. The number distribution of particle size as measured with NTA indicated homogenous population of particles with the average diameter of ~210 nm for both blank DOTAP–HA NPs and OVA-DOTAP–HA NPs (Fig. 4), thus corroborating the results of the DLS analyses of the particles.

Notably, DOTAP liposomes loaded with OVA immediately formed aggregates after resuspension in PBS (data not shown), whereas OVA-DOTAP–HA NPs stably maintained their size distribution even after 3 days of incubation at 37 °C (Fig. S1). Next, we examined antigen release from DOTAP–HA NPs loaded with Texas Red-labeled OVA (we omitted the DOTAP liposome group due to aggregation). When incubated in 10% FBS containing media at 37 °C, OVA-DOTAP–HA NPs steadily released ~40% of encapsulated OVA over 3 weeks, demonstrating stability of the NPs (Fig. 5).

3.3. Activation of BMDCs with adjuvant-loaded DOTAP–HA NPs

Maturation of dendritic cells (DCs) involves up-regulation of a series of cell surface markers [35], including co-stimulatory molecules CD40 and CD80/86, and MHC-II responsible for antigen presentation to $CD4^+$ T cells. We investigated DC activation by incubating BMDCs with different particle formulations (Fig. 6). After overnight culture, BMDCs exhibited minor increase in the expression levels of CD86 and MHC-II after treatment with OVA-DOTAP liposomes. Treatment with OVA-DOTAP–HA NPs also led to slight increase in the expression levels of MHC-II, indicating low immunogenicity of particles without any danger signals. To promote DC maturation, we incorporated MPLA, a FDA-approved TLR4 agonist, into DOTAP–HA NPs by adding MPLA into the initial lipid film prior to hydration. Compared with OVA-DOTAP–HA NPs, DOTAP–HA NPs co-loaded with OVA and MPLA significantly up-regulated CD40 (Fig. 6a), CD86 (Fig. 6b) and MHC-II (Fig. 6c) on DCs, indicating the immunostimulatory property of MPLA-loaded DOTAP–HA NPs.

3.4. Enhanced biocompatibility DOTAP–HA NPs, compared with DOTAP liposomes

One of the major concerns of using DOTAP as a delivery vehicle is its widely reported cytotoxicity [9,10]. To compare cytotoxicity of DOTAP liposomes and DOTAP–HA NPs, we pulsed BMDCs with various concentrations of OVA-DOTAP liposomes or OVA-DOTAP–HA NPs with or without MPLA. Measurement of cell viability after overnight culture indicated that OVA-DOTAP liposome formulations with or without MPLA induced significant BMDC cytotoxicity with 50% of cell death observed at LC_{50} value of ~0.2 mg/ml (Fig. 7). In contrast, BMDCs were able to

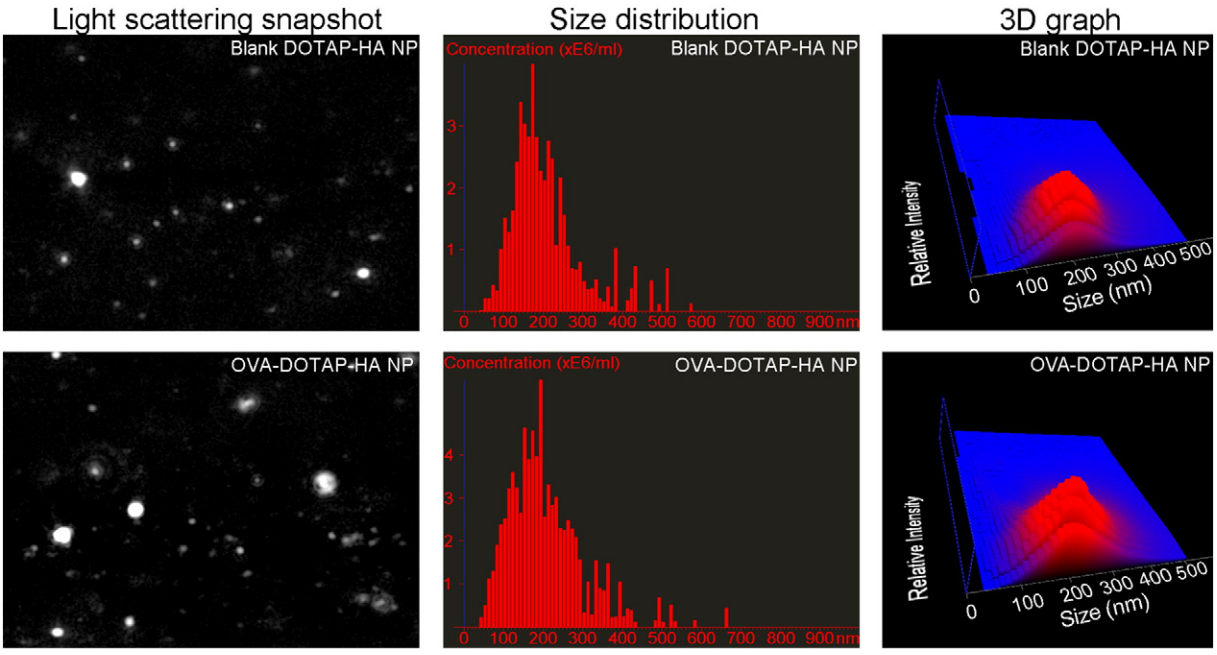

Fig. 4. Nanoparticle tracking analysis of DOTAP–HA NP. Representative NTA video frame (left panel), size distribution (middle panel), and 3D graph (right panel showing size vs. light scattering intensity vs. particle concentration) are shown for blank and OVA-containing DOTAP–HA NPs.

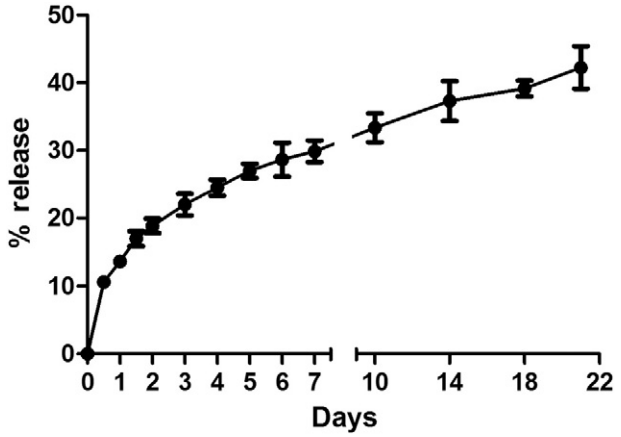

Fig. 5. Steady release of protein antigen from DOTAP–HA NPs. DOTAP–HA NPs encapsulating Texas Red-labeled OVA were loaded in dialysis cassettes (MWCO 300 kDa) and incubated in RPMI 1640 supplemented with 10% FBS at 37 °C under constant shaking. Protein release was quantified by measuring fluorescence intensity of release media over 3 weeks with excitation/emission wavelengths of 585/615 nm. Results are mean ± SEM (n = 3).

tolerate at least 20-fold higher concentration of lipids in OVA-DOTAP–HA NPs (LC_{50} > 4 mg/ml). In addition, BMDCs exhibited similar levels of viability when incubated with DOTAP–HA NPs with or without PEGylation (Fig. S2). These results showed that ionic complexation of DOTAP liposomes with HA biopolymer significantly enhanced their biocompatibility. Overall, liposome-HA hybrid NPs potently activated DCs with significantly reduced cytotoxicity, compared with DOTAP liposomes.

3.5. Vaccination with DOTAP–HA NPs elicits adaptive immune responses

Next, we investigated the induction of humoral and cellular immune responses after intranasal delivery of OVA and MPLA in either soluble form or DOTAP–HA NPs. C57BL/6 mice were immunized with 50 μg of OVA and 0.58 μg of MPLA either in solution or DOTAP–HA NPs via intranasal administration on days 0 and 28. Immune sera were collected on days 21 and 49, 3 weeks post-prime and boost, respectively, and analyzed for OVA-specific IgG responses with ELISA. Immunization with OVA/MPLA-DOTAP–HA NPs elicited significantly enhanced OVA-specific IgG responses, compared with immunization with soluble vaccines (Fig. 8a). Among IgG subtypes, a robust level of OVA-specific IgG_1 response was observed in mice immunized with OVA/MPLA-DOTAP–HA NPs (Fig. 8b); however, IgG_{2c} responses were not detected in any of the groups (Fig. 8c), indicating strong skewing toward Th2 over Th1 humoral immune responses with the OVA antigen.

We also examined elicitation of OVA-specific cellular immune responses by assessing the frequency of OVA-specific $CD8^+$ T cells among PBMCs on day 7 after vaccination (Fig. 9). Compared with the PBS group, vaccination with DOTAP–HA NPs significantly increased the frequency of OVA-specific $CD8^+$ T cells among PBMCs as measured with fluorophore-conjugated tetramer with $OVA_{257–264}$ (SIINFEKL) in the context of H-$2K^b$. Although the difference was not statistically significant, there was a trend for increased OVA-specific $CD8^+$ T cell responses in the DOTAP–HA NP group, compared with the soluble vaccine group. Overall, intranasal vaccination with DOTAP–HA NPs enhanced both B- and T-cell immune responses, compared with the equivalent dose of soluble vaccines.

In addition, we examined whether intranasal vaccination leads to systemic delivery of vaccine components. C57BL/6 mice were administered with Texas Red-labeled OVA in either free soluble form or DOTAP–HA NPs, and after 4 h we examined the heart, lungs, spleen, liver, and kidneys for the presence of OVA by measuring the fluorescence signal. We did not detect any accumulation of OVA in any of the major organs after intranasal vaccination with free OVA or OVA-DOTA–HA NPs (Fig. S3). In contrast, as we expected, intravenous injection of the same dose of OVA-DOTAP–HA NPs resulted in robust accumulation in the liver. These results suggest that there is minimal penetration of vaccine components into systemic compartments after intranasal administration, at least for the time window that we examined in our studies.

3.6. Intranasal vaccination with DOTAP–HA NPs elicits robust humoral immune responses against F1-V

DOTAP–HA NPs were also used to deliver F1-V via intranasal route of vaccination. C57BL/6 mice were immunized with F1-V and MPLA either in soluble form or DOTAP–HA NPs, and the immune sera were analyzed for F1-V specific antibody titers. The prime and first boost doses given on day 0 and 28 contained 1 μg F1-V and 0.58 μg MPLA per mouse. Although there was a detectable increase in anti-F1-V IgG titers after the first boost immunization, due to low overall IgG responses, we decided to increase the second booster dose to 5 μg F1-V and 2.9 μg MPLA per mouse to ensure sero-conversion and to more clearly distinguish the potency of soluble vs. particulate vaccine formulations. After the second booster doses, the hybrid NP delivery system elicited substantially higher F1-V-specific total IgG titers, compared with soluble F1-V vaccines (11-fold increase on day 77, $p < 0.0001$, Fig. 10a). Analyses of F1-V-specific IgG_1 (Fig. 10b) and IgG_{2c} (Fig. 10c) responses also revealed

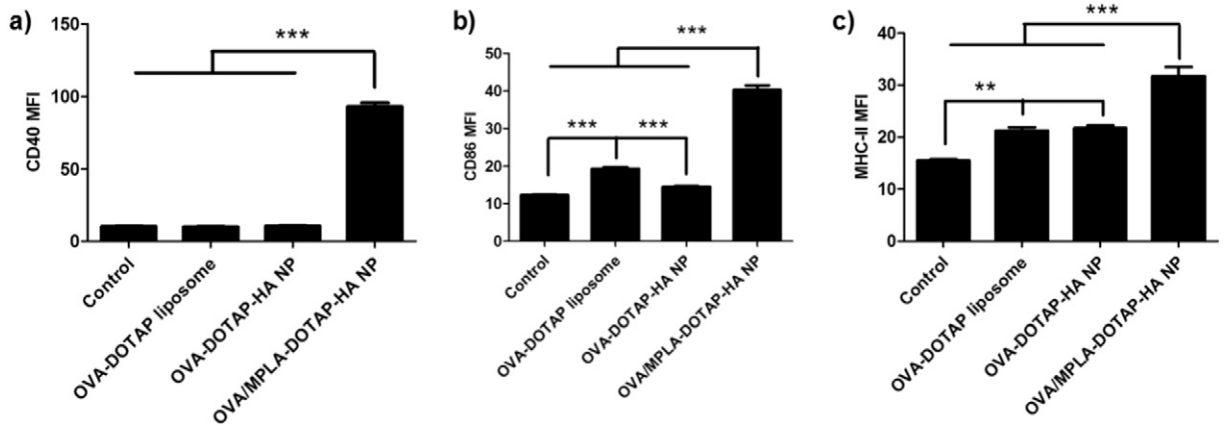

Fig. 6. MPLA-loaded DOTAP–HA NPs induce maturation of BMDCs. BMDCs were pulsed with DOTAP liposomes or DOTAP–HA NPs with 5 μg/ml of OVA with or without 0.58 μg/ml of MPLA for 2 h at 37 °C. After overnight culture, expression levels of CD40 (a), CD86 (b) and MHC-II (c) were measured by flow cytometry. BMDCs treated with culture media served as the negative control. $^{**}p < 0.01$ and $^{***}p < 0.001$, as analyzed by one-way ANOVA followed by Bonferroni's test for comparison of multiple groups. Results are mean fluorescence intensity (MFI) ± SEM (n = 6).

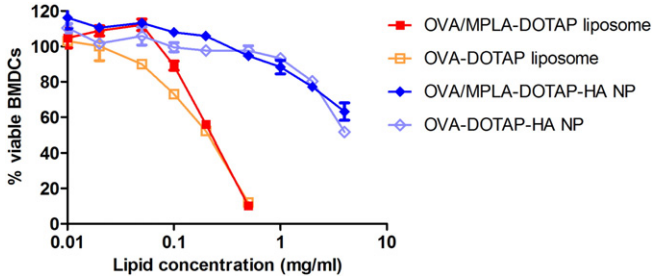

Fig. 7. Cytotoxicity of DOTAP liposomes and DOTAP–HA NPs. BMDCs were pulsed with OVA-DOTAP liposomes or OVA-DOTAP–HA NPs with or without MPLA for 2 h at 37 °C. After overnight culture, BMDC viability was measured with a CCK-8 kit and reported as the percentage of viable BMDCs relative to the media treatment control group. Results are reported as mean ± SEM (n = 3).

similar trend with 23-fold ($p < 0.05$) and 15-fold increases ($p < 0.001$) in sera titers on day 77, compared with immune sera from mice immunized with soluble F1-V vaccines. Notably, IgG_1 responses induced by DOTAP–HA NPs reached their peak on day 63 (1 week post the second boost) and started to decrease by day 77. On the other hand, IgG_{2c} responses continued to increase after the second boost and reached substantially enhanced sera titer by day 77, contributing to the overall anti-F1-V total IgG titer. Thus, unlike the case with the OVA antigen (Fig. 8), F1-V delivered by DOTAP–HA NPs exhibited Th1/Th2-balanced humoral immune responses, suggesting that the identity of subunit antigen formulated into these vaccine NPs may have a direct impact on the Th1/Th2 humoral immune responses.

4. Discussion

In this work, we have utilized the ionic interaction between cationic DOTAP liposomes and anionic HA to form lipid–polymer hybrid NPs and examined their efficacy as delivery vehicles for protein antigens and immunostimulatory agents in vitro and in vivo. Our results indicated that DOTAP–HA NPs carrying MPLA, a TLR4 agonist, significantly improved BMDC activation while reducing cytotoxicity of DOTAP-based liposomes by at least 20-fold as indicated by their LC_{50} values. In addition, when administered via intranasal route, these vaccine NPs elicited significantly enhanced humoral immune responses against subunit protein antigens, compared with soluble vaccine formulations. Importantly, F1-V, a candidate antigen for *Y. pestis* was successfully formulated into DOTAP–HA NPs, and intranasal vaccination with these NPs induced substantially enhanced antigen-specific IgG titers with

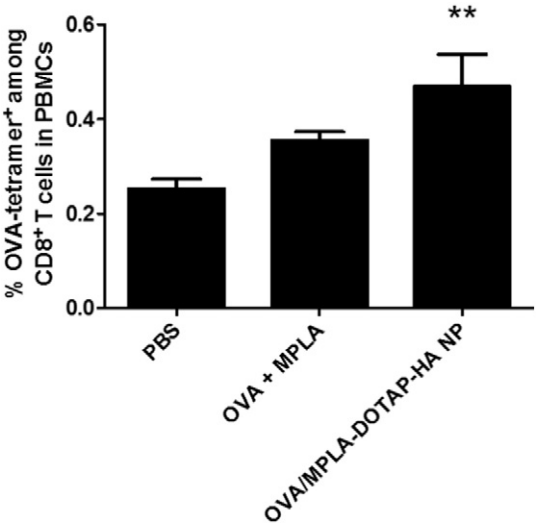

Fig. 9. Vaccination with DOTAP–HA NPs elicits antigen-specific cellular immune responses. C57BL/6 mice were immunized via intranasal route with PBS or OVA and MPLA either in free soluble form or in DOTAP–HA NPs (OVA dose: 50 μg/mouse; MPLA dose: 0.58 μg/mouse). PBMCs were collected on day 7 and analyzed for OVA-specific $CD8^+$ T cells by tetramer staining and flow cytometry. $^{**}p < 0.01$ in comparison to PBS control, as analyzed by one-way ANOVA, followed by Bonferroni's test for comparison of multiple groups. Results are reported as mean ± SEM (n = 7).

balanced Th1/Th2 IgG responses, compared with the soluble vaccine counterpart, suggesting their potential as a pulmonary vaccine platform.

Liposomal fusion can be induced by the ionic interaction between lipids and charged small molecules such as Ca^{2+}, Mg^{2+} [36,37], fusogenic peptides [38], or polymers such as dextran sulfate [39], poly(malic acid) [30] and polylysine [40]. In this study, we report that HA and its thiolated form can induce fusion of cationic DOTAP-containing liposomes. This is supported by our results from the DLS (Fig. 2) and FRET (Fig. 3) assays that revealed efficient complexation of cationic liposomes with HA polymer (polymer: total lipid = 1:10, w/w). In addition, incorporation of DOTAP liposomes with thiolated HA polymers allows for facile surface modification of the particles with thiol-PEG, and our quantification of PEG content with barium iodide (Table 1) confirmed the presence of PEG outer shell layer on NPs. Overall our results indicate that DOTAP/HA core-PEG shell NPs are stable in PBS and serum-containing media, allowing for prolonged release of protein antigen over at least 3 weeks at 37 °C (Figs. S1 and 5).

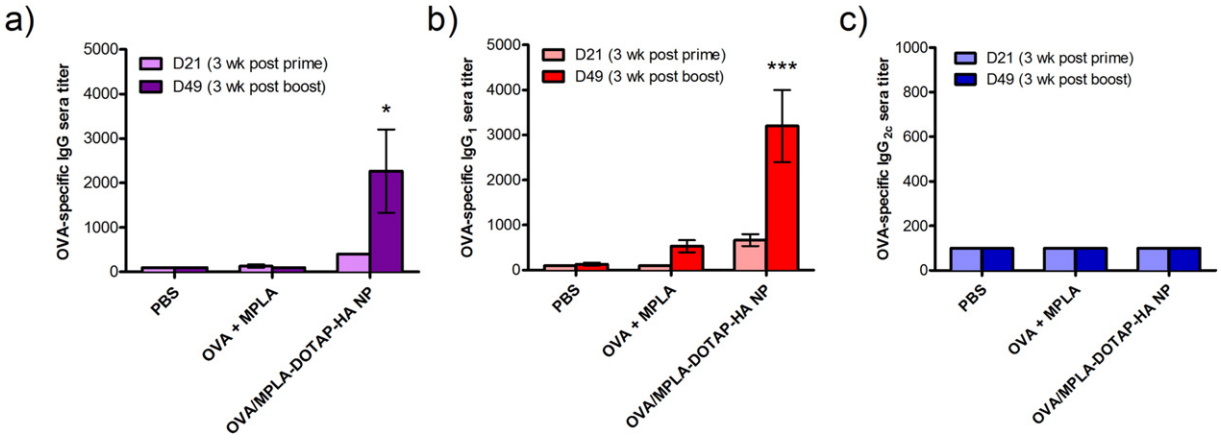

Fig. 8. Vaccination with DOTAP–HA NPs elicits antigen-specific humoral immune responses. C57BL/6 mice were vaccinated with PBS, soluble OVA plus MPLA, or OVA and MPLA co-loaded in DOTAP–HA NPs on days 0 and 28 via intranasal route (OVA dose: 50 μg/mouse; MPLA dose: 0.58 μg/mouse). Sera samples were collected on days 21 and 49 for analysis of OVA-specific total IgG (a), IgG_1 (b) and IgG_{2c} (c) titers by ELISA. $^{*}p < 0.05$ and $^{***}p < 0.001$ in comparison to PBS and solution groups on day 49, as analyzed by two-way ANOVA, followed by Bonferroni's test for comparison of multiple groups. Results are reported as mean ± SEM (n = 3).

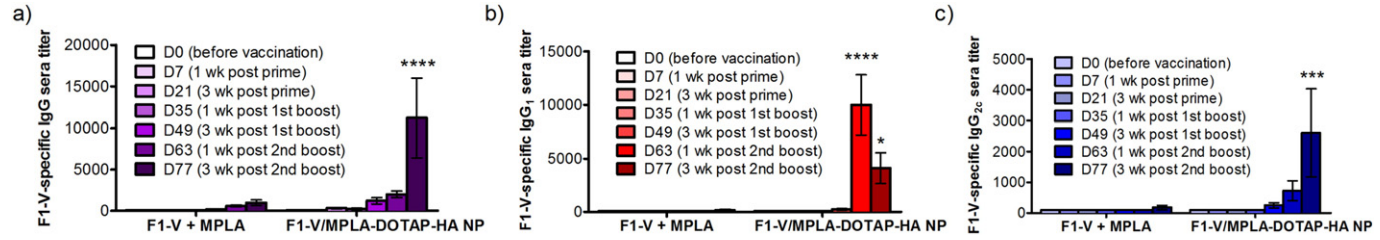

Fig. 10. Vaccination with DOTAP–HA NPs induces F1-V-specific humoral immune responses. C57BL/6 mice were intranasally immunized with free F1-V and MPLA, or F1-V and MPLA co-loaded DOTAP–HA NPs on days 0 and 28 (F1-V dose: 1 μg/mouse; MPLA dose: 0.58 μg/mouse). The second booster dose given on day 56 was increased to 5 μg F1-V and 2.9 μg MPLA to ensure successful sero-conversion. Sera were collected on days 0, 7, 21, 35, 49, 63 and 77 and analyzed for F1-V-specific total IgG (a), IgG_1 (b) and IgG_{2c} (c) titers by ELISA. $^{*}p < 0.05$, $^{***}p < 0.001$ and $^{****}p < 0.0001$ in comparison to the soluble F1-V plus MPLA group of the same time point, as analyzed by two-way ANOVA, followed by Bonferroni's test for comparison of multiple groups. Results are reported as mean ± SEM (n = 4).

DCs are considered to be the most efficient antigen-presenting cells that play a key role in both innate and adaptive immune responses. During DC maturation, elevated MHC-II presents antigens to $CD4^+$ T cells (signal 1), while CD80/86 provides necessary co-stimulatory signal 2 for T cell activation. Increased CD40 is also necessary for DCs to receive further activation signals from $CD4^+$ T helper cells. Blank DOTAP liposomes and DOTAP–HA NPs without any other danger signal did not lead to any appreciable activation of DCs beyond the PBS control group, whereas incorporation of MPLA into DOTAP–HA NPs resulted in efficient promotion of DC maturation. In addition, compared with DOTAP liposomes, DOTAP–HA NPs exhibited significantly reduced cytotoxicity in BMDC culture (Fig. 7). In line with enhanced DC activation and reduced cytotoxicity, DOTAP–HA NPs co-loaded with OVA and MPLA stimulated stronger adaptive cellular and humoral immune responses following intranasal immunization in vivo. Similar advantages have been reported in nasal immunization with nanoparticles composed of other biodegradable polymers, such as trimethyl chitosan which increased sera anti-OVA IgG titers [16,41] and poly(γ-glutamic acid) which enhanced OVA-specific CD8 T cell response [42]. In our current studies, we have shown that DOTAP–HA NPs are a potent vaccine delivery system that can induce concerted, antigen-specific cellular and humoral immune responses. These results formed the basis for our studies investigating the efficacy of our particles for intranasal vaccination with F1-V.

As pneumonic plague can be easily transmitted by respiratory tract with deadly consequences, nasal vaccination has been the subject of various prior studies. A previous study comparing various routes of vaccination has reported that intranasal vaccination with F1-V resulted in humoral immune responses comparable to subcutaneous or intramuscular immunizations [43,44]. Moreover, adjuvants were shown to be indispensable for protection against *Y. pestis* infection by intranasal immunization of F1-V [45]. Recently, F1-V and MPLA have been intranasally delivered by polyanhydride nanoparticles, resulting in significantly improved lung residence of F1-V and plague protection [22,23]. These results highlight the benefits of particulate delivery system for F1-V vaccine. In our current studies, intranasal vaccination with DOTAP–HA NPs co-encapsulating F1-V and MPLA led to substantially enhanced F1-V-specific humoral immune responses, compared with immunization with soluble F1-V and MPLA vaccine. Notably, we were able to achieve successful sero-conversion and balanced Th1/Th2 humoral immune responses against F1-V using low doses of F1-V (1–5 μg) formulated into NPs, whereas the equivalent vaccine dose in soluble formulation failed to elicit humoral immune responses above the basal level. These results highlight the potency of DOTAP–HA NPs to generate immune responses against F1-V with significant dose sparing, compared with conventional vaccine formulations. Our future studies will be directed to provide mechanistic insights into the process of NP-mediated antigen delivery to antigen-presenting cells within nasal-associated lymphoid tissues and to delineate the impact of IgG_1/IgG_{2c}-balanced humoral immune responses on protection against *Y. pestis* infection. Collectively, these results suggest that DOTAP–HA NPs may serve as a promising vaccine delivery platform for intranasal vaccination against *Y. pestis*.

5. Conclusion

Liposome–polymer hybrid NPs were constructed and tested as a nasal vaccine delivery system. Cationic DOTAP liposomes were incorporated with HA and PEGylated for enhanced biocompatibility, improved colloidal stability, and steady antigen release. These NPs co-loaded with protein antigen and adjuvant molecules more efficiently promoted DC maturation and stimulated stronger humoral and cellular immune responses, compared with soluble vaccine formulations. Intranasal vaccination with NPs carrying F1-V antigen and MPLA led to robust serum IgG responses, characterized by Th1/Th2-balanced humoral immune responses, indicating the potential of the hybrid DOTAP–HA NP system for prophylactic vaccination against infectious pathogens.

Acknowledgment

This study was supported by the National Institute of Health grant 1K22AI097291-01 and by the National Center for Advancing Translational Sciences of the National Institutes of Health under Award Number UL1TR000433. *Yersinia pestis* F1-V fusion protein, recombinant from *Escherichia coli* (#NR-4526), was obtained through the NIH Biodefense and Emerging Infections Research Resources Repository, NIAID, NIH. We also thank Prof. Dennis W. Metzger at Albany Medical College for discussion of our work.

Appendix A. Supplementary data

Supplementary data to this article can be found online at http://dx.doi.org/10.1016/j.jconrel.2015.04.010.

References

[1] D.J. Irvine, M.A. Swartz, G.L. Szeto, Engineering synthetic vaccines using cues from natural immunity, Nat. Mater. 12 (2013) 978–990.
[2] J.J. Moon, B. Huang, D.J. Irvine, Engineering nano- and microparticles to tune immunity, Adv. Mater. 24 (2012) 3724–3746.
[3] P. Sahdev, L.J. Ochyl, J.J. Moon, Biomaterials for nanoparticle vaccine delivery systems, Pharm. Res. 31 (2014) 2563–2582.
[4] G. Gregoriadis, R. Saffie, J.B. de Souza, Liposome-mediated DNA vaccination, FEBS Lett. 402 (1997) 107–110.
[5] Y. Perrie, P.M. Frederik, G. Gregoriadis, Liposome-mediated DNA vaccination: the effect of vesicle composition, Vaccine 19 (2001) 3301–3310.
[6] W. Yan, W. Chen, L. Huang, Reactive oxygen species play a central role in the activity of cationic liposome based cancer vaccine, J. Control. Release 130 (2008) 22–28.
[7] W. Chen, W. Yan, L. Huang, A simple but effective cancer vaccine consisting of an antigen and a cationic lipid, Cancer Immunol. Immunother. 57 (2008) 517–530.
[8] D. Christensen, K.S. Korsholm, P. Andersen, E.M. Agger, Cationic liposomes as vaccine adjuvants, Expert Rev. Vaccines 10 (2011) 513–521.
[9] K. Lappalainen, I. Jaaskelainen, K. Syrjanen, A. Urtti, S. Syrjanen, Comparison of cell proliferation and toxicity assays using two cationic liposomes, Pharm. Res. 11 (1994) 1127–1131.

[10] H. Lv, S. Zhang, B. Wang, S. Cui, J. Yan, Toxicity of cationic lipids and cationic polymers in gene delivery, J. Control. Release 114 (2006) 100–109.
[11] J.J. Moon, H. Suh, A. Bershteyn, M.T. Stephan, H. Liu, B. Huang, M. Sohail, S. Luo, S.H. Um, H. Khant, J.T. Goodwin, J. Ramos, W. Chiu, D.J. Irvine, Interbilayer-crosslinked multilamellar vesicles as synthetic vaccines for potent humoral and cellular immune responses, Nat. Mater. 10 (2011) 243–251.
[12] P.C. DeMuth, J.J. Moon, H. Suh, P.T. Hammond, D.J. Irvine, Releasable layer-by-layer assembly of stabilized lipid nanocapsules on microneedles for enhanced transcutaneous vaccine delivery, ACS Nano 6 (2012) 8041–8051.
[13] A.V. Li, J.J. Moon, W. Abraham, H. Suh, J. Elkhader, M.A. Seidman, M. Yen, E.J. Im, M.H. Foley, D.H. Barouch, D.J. Irvine, Generation of effector memory T cell-based mucosal and systemic immunity with pulmonary nanoparticle vaccination, Sci. Transl. Med. 5 (2013) 204ra130.
[14] A.A. Gasperini, X.E. Puentes-Martinez, T.A. Balbino, T. de Paula Rigoletto, G. de Sa Cavalcanti Correa, A. Cassago, R.V. Portugal, L.G. de La Torre, L.P. Cavalcanti, Association between cationic liposomes and low molecular weight hyaluronic acid, Langmuir 31 (2015) 3308–3317.
[15] M. Singh, M. Briones, D.T. O'Hagan, A novel bioadhesive intranasal delivery system for inactivated influenza vaccines, J. Control. Release 70 (2001) 267–276.
[16] R.J. Verheul, B. Slutter, S.M. Bal, J.A. Bouwstra, W. Jiskoot, W.E. Hennink, Covalently stabilized trimethyl chitosan-hyaluronic acid nanoparticles for nasal and intradermal vaccination, J. Control. Release 156 (2011) 46–52.
[17] R.J. Verheul, S. van der Wal, W.E. Hennink, Tailorable thiolated trimethyl chitosans for covalently stabilized nanoparticles, Biomacromolecules 11 (2010) 1965–1971.
[18] L.E. Quenee, N.A. Ciletti, D. Elli, T.M. Hermanas, O. Schneewind, Prevention of pneumonic plague in mice, rats, guinea pigs and non-human primates with clinical grade rV10, rV10-2 or F1-V vaccines, Vaccine 29 (2011) 6572–6583.
[19] N. Csaba, M. Garcia-Fuentes, M.J. Alonso, Nanoparticles for nasal vaccination, Adv. Drug Deliv. Rev. 61 (2009) 140–157.
[20] D.G. Heath, G.W. Anderson Jr., J.M. Mauro, S.L. Welkos, G.P. Andrews, J. Adamovicz, A.M. Friedlander, Protection against experimental bubonic and pneumonic plague by a recombinant capsular F1-V antigen fusion protein vaccine, Vaccine 16 (1998) 1131–1137.
[21] S. Uddowla, L.C. Freytag, J.D. Clements, Effect of adjuvants and route of immunizations on the immune response to recombinant plague antigens, Vaccine 25 (2007) 7984–7993.
[22] K.A. Ross, S.L. Haughney, L.K. Petersen, P. Boggiatto, M.J. Wannemuehler, B. Narasimhan, Lung deposition and cellular uptake behavior of pathogen-mimicking nanovaccines in the first 48 hours, Adv. Healthc. Mater. 3 (2014) 1071–1077.
[23] B.D. Ulery, D. Kumar, A.E. Ramer-Tait, D.W. Metzger, M.J. Wannemuehler, B. Narasimhan, Design of a protective single-dose intranasal nanoparticle-based vaccine platform for respiratory infectious diseases, PLoS One 6 (2011) e17642.
[24] B. Guy, The perfect mix: recent progress in adjuvant research, Nat. Rev. Microbiol. 5 (2007) 505–517.
[25] C.R. Alving, M. Rao, N.J. Steers, G.R. Matyas, A.V. Mayorov, Liposomes containing lipid A: an effective, safe, generic adjuvant system for synthetic vaccines, Expert Rev. Vaccines 11 (2012) 733–744.
[26] V. Filipe, A. Hawe, W. Jiskoot, Critical evaluation of Nanoparticle Tracking Analysis (NTA) by NanoSight for the measurement of nanoparticles and protein aggregates, Pharm. Res. 27 (2010) 796–810.
[27] G.E. Sims, T.J. Snape, A method for the estimation of polyethylene glycol in plasma protein fractions, Anal. Biochem. 107 (1980) 60–63.
[28] X.W. Gong, D.Z. Wei, M.L. He, Y.C. Xiong, Discarded free PEG-based assay for obtaining the modification extent of pegylated proteins, Talanta 71 (2007) 381–384.
[29] D. Hoekstra, Role of lipid phase separations and membrane hydration in phospholipid vesicle fusion, Biochemistry 21 (1982) 2833–2840.
[30] S. Osanai, K. Nakamura, Effects of complexation between liposome and poly(malic acid) on aggregation and leakage behaviour, Biomaterials 21 (2000) 867–876.
[31] C. Berney, G. Danuser, FRET or no FRET: a quantitative comparison, Biophys. J. 84 (2003) 3992–4010.
[32] M.B. Lutz, N. Kukutsch, A.L. Ogilvie, S. Rossner, F. Koch, N. Romani, G. Schuler, An advanced culture method for generating large quantities of highly pure dendritic cells from mouse bone marrow, J. Immunol. Methods 223 (1999) 77–92.
[33] M. Ishiyama, Y. Miyazono, K. Sasamoto, Y. Ohkura, K. Ueno, A highly water-soluble disulfonated tetrazolium salt as a chromogenic indicator for NADH as well as cell viability, Talanta 44 (1997) 1299–1305.
[34] L.J. Ochyl, J.J. Moon, Whole-animal imaging and flow cytometric techniques for analysis of antigen-specific CD8$^+$ T cell responses after nanoparticle vaccination, J. Vis. Exp. (2015) e52771, http://dx.doi.org/10.3791/52771.
[35] J. Banchereau, A.K. Palucka, Dendritic cells as therapeutic vaccines against cancer, Nat. Rev. Immunol. 5 (2005) 296–306.
[36] D.C. Miller, G.P. Dahl, Early events in calcium-induced liposome fusion, Biochim. Biophys. Acta 689 (1982) 165–169.
[37] D. Papahadjopoulos, S. Nir, N. Duzgunes, Molecular mechanisms of calcium-induced membrane fusion, J. Bioenerg. Biomembr. 22 (1990) 157–179.
[38] Y. Xia, J. Sun, D. Liang, Aggregation, fusion, and leakage of liposomes induced by peptides, Langmuir 30 (2014) 7334–7342.
[39] K. Arnold, S. Ohki, M. Krumbiegel, Interaction of dextran sulfate with phospholipid surfaces and liposome aggregation and fusion, Chem. Phys. Lipids 55 (1990) 301–307.
[40] A.A. Yaroslavov, A.V. Sybachin, E. Kesselman, J. Schmidt, Y. Talmon, S.A. Rizvi, F.M. Menger, Liposome fusion rates depend upon the conformation of polycation catalysts, J. Am. Chem. Soc. 133 (2011) 2881–2883.
[41] B. Slutter, S. Bal, C. Keijzer, R. Mallants, N. Hagenaars, I. Que, E. Kaijzel, W. van Eden, P. Augustijns, C. Lowik, J. Bouwstra, F. Broere, W. Jiskoot, Nasal vaccination with N-trimethyl chitosan and PLGA based nanoparticles: nanoparticle characteristics determine quality and strength of the antibody response in mice against the encapsulated antigen, Vaccine 28 (2010) 6282–6291.
[42] T. Uto, X. Wang, T. Akagi, R. Zenkyu, M. Akashi, M. Baba, Improvement of adaptive immunity by antigen-carrying biodegradable nanoparticles, Biochem. Biophys. Res. Commun. 379 (2009) 600–604.
[43] A. Glynn, L.C. Freytag, J.D. Clements, Effect of homologous and heterologous prime-boost on the immune response to recombinant plague antigens, Vaccine 23 (2005) 1957–1965.
[44] T. Jones, J.J. Adamovicz, S.L. Cyr, C.R. Bolt, N. Bellerose, L.M. Pitt, G.H. Lowell, D.S. Burt, Intranasal Protollin/F1-V vaccine elicits respiratory and serum antibody responses and protects mice against lethal aerosolized plague infection, Vaccine 24 (2006) 1625–1632.
[45] A. Glynn, C.J. Roy, B.S. Powell, J.J. Adamovicz, L.C. Freytag, J.D. Clements, Protection against aerosolized *Yersinia pestis* challenge following homologous and heterologous prime-boost with recombinant plague antigens, Infect. Immun. 73 (2005) 5256–5261.